Research Journal of Applied Sciences, Engineering and Technology 5(10): 2934-2940, 2013
DOI:10.19026/rjaset.5.4602
ISSN: 2040-7459; e-ISSN: 2040-7467

Submitted: September 13, 2012 Accepted: September 19, 2012 Published: March 25, 2013

Research Article

Prediction of Welding Deformation and Residual Stresses in Fillet Welds Using Indirect Couple Field FE Method

[1]Asifa Khurram, [2]Li Hong, [1]Li Li and [3]Khurram Shehzad
[1]College of Materials Science and Chemical Engineering,
[2]College of Aerospace and Civil Engineering,
[3]College of Shipbuilding Engineering, Harbin Engineering University, Harbin 150001, China

Abstract: Fillet welds are extensively used in shipbuilding, automobile and other industries. Heat concentrated at a small area during welding induces distortions and residual stresses, affecting the structural strength. In this study, indirect coupled-field method is used to predict welding residual stresses and deformation in a fillet joint due to welding on both sides. 3-D nonlinear thermal finite element analysis is performed in ANSYS software followed by a structural analysis. Symmetrical boundary conditions are applied on half of the model for simplification. Results of FE structure analysis predict residual stresses in the specimen. A comparison of simulation results with experimental values proves the authenticity of the technique. The present study can be extended for complex structures and welding techniques.

Keywords: Couple field, finite element method, fillet weld, residual stresses, symmetrical boundary condition

INTRODUCTION

Fillet joints are widely used in bridges and ship structures. Fillet welded joints usually suffer various welding deformation patterns such as longitudinal shrinkage, transverse shrinkage, angular distortion and bending. The concentrated thermal gradient followed by cooling during the welding process induces residual stresses and distortions. Excessive distortions of welded components have negative effects on fabrication accuracy, external appearance and various strengths of the structures. Various corrective measures like post weld heat treatment, flame straightening, vibratory stress relief, induction heat treatment and cold bending can be used to lower the distortion level. However, these methods are costly and time consuming. Welding induced residual stresses may cause early yielding and reduce buckling strength. Therefore, prediction and control of welding deformation and residual stresses is critical to improve the quality and reliability of the structure. Withers and Bhadeshia (2001) defined residual stresses and summarized their measurement techniques. Experimental methods for the prediction of residual stress include stress relaxation, x-ray diffraction, ultrasonic and cracking (Teng *et al*., 2001). All these methods are either destructive or expensive, which drive the requirement of simulation techniques.

A weld simulation model involves geometrical constraints, material nonlinearities, all physical phenomena and welding parameters such as welding speed, current, voltage, efficiency. Improved and complex simulation models also include number and sequence of passes and filler material. Researchers have been working in the field of computational welding mechanics in order to accurately predict welding residual stresses and deformations (Goldak 2005; Lindgren and Karlsson, 1988; Lindgren, 2001).

Welding process is treated as a transient nonlinear problem in finite element thermo-elastic–plastic analysis. Camilleri *et al*. (2003, 2005) computed welding temperature field by FE methods and validated the results by experiments. Lee *et al*. (2008), Ueda *et al*. (1988), Ueda and Yuan (1993) and Barroso *et al*. (2010) predicted the effect of different shapes and material properties on welding residual stresses and distortions. Mollicone *et al*. (2006) described modeling strategies to simulate the thermo-elastic-plastic stages of the welding process and compared FE model with experiments. Iranmanesh and Darvazi (2008) presented a FE based calculation process to study temperature field and residual stresses using 2 and 3-dimensional models in ANSYS 9.0.

Gao and Zhang (2011) addressed moving heat source, latent heat of phase change and characteristic parameters of materials in the simulation model. Moraitis and Labeas (2009) developed a 3D FE model to predict keyhole formation and thermo-mechanical response during laser beam welding of steel and

Corresponding Author: Asifa Khurram, College of Materials Science and Chemical Engineering, Harbin Engineering University, Harbin 150001, China

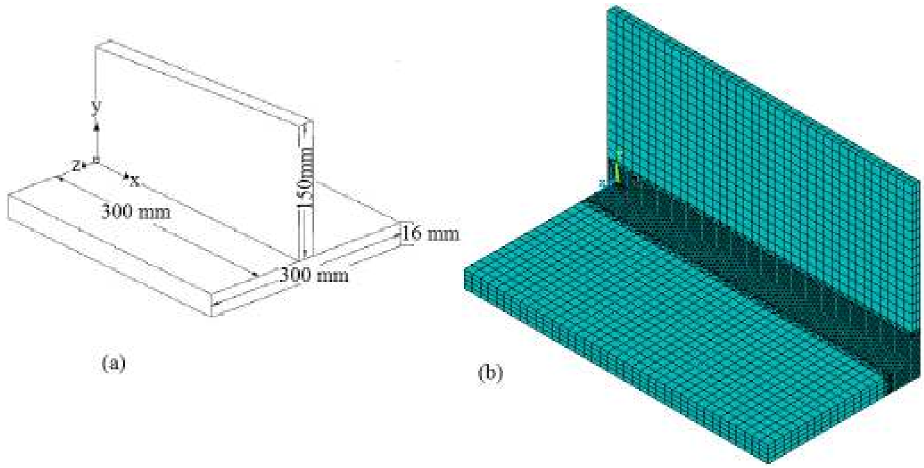

Fig. 1: (a) Model geometry (b) Simplified FE model

aluminum pressure vessel or pipe butt-joints. Xu *et al*. (2008) presented the FE method based on the inherent strain theory to simulate welding distortion in multi-pass girth butt welded pipes of different wall thickness. Sulaiman *et al*. (2011) investigated the capability of linear thermal elastic numerical analysis to predict the welding distortion due to GMAW by FEM software WELDPLANNER. Mrvar *et al*. (2011) simulated welding of pipe with finite element program SYSWELD.

In this study, temperature distribution due to fillet welding on both sides of the web is calculated at each load step followed by structure analysis using the temperature field data. It is assumed that the structural results do not affect the thermal analysis.Therefore, only unidirectional coupling is carried out. Experiments are performed to validate the simulation results.The computed deformations are compared with experimental results measured at several point and residual stresses are predicted.

SIMULATION METHOD

FE modeling: Model geometry used in this study is shown in Fig.1a. Material of both flange and web is low carbon steel. For FE analysis the half of the model is considered and symmetric boundary conditions are applied. The temperature gradient is considerably lower in the regions away from the weld location. Therefore, bigger element size is used to reduce the number of degrees of freedom and the computation time (Fig. 1b).

Thermal analysis: Non-linear thermal analysis is conducted using solid 70, eight node brick elements. Welding arc is considered as a moving surface heat source. Temperature history of the plate is evaluated using three dimensional transient thermal analysis.

Table 1: Welding parameters

Welding speed mm/sec	Efficiency (%)	Current (A)	Voltage (V)	Torch angle
5	80	300	30	45°

Heat source model: In this study, at any time t, the heat of the welding arc is modeled by a surface heat source with a Gaussian distribution (Gao and Zhang, 2011). Thus, points lying on the surface of the work piece within the arc beam radius r_a receive distributed heat fluxes q_t as follows:

$$\boldsymbol{q_t = \frac{3Q}{\pi r_a^2} exp\left[-\left(\frac{r_a}{r_t}\right)^2\right]} \tag{1}$$

where, r_t is the radial distance measured from the instantaneous arc center on the surface of the work piece and Q is the heat input from the welding arc. Where Q = ηVI is the energy of the welding arc, η is the arc efficiency, V is voltage and I is the welding current respectively. The value of welding parameters are given in Table 1.

Heat transfer model: Equation (2) is the governing Eq. of 3D transient heat transfer in such methods while Eq. (3) represents the heat loss due to convection and radiation.

$$k\frac{\delta^2 T}{\delta x^2} + k\frac{\delta^2 T}{\delta y^2} + k\frac{\delta^2 T}{\delta z^2} + \frac{\delta Q}{\delta x^2} = \rho C\frac{\delta T}{\delta t} \tag{2}$$

$$h(T - T_0) + \beta \in (T^4 - T_0^4) = q_s \tag{3}$$

where Q is the internal heat energy released or consumed per unit volume (J/mm^3), q_s is the heat loss, T is temperature, T_0 is ambient temperature, t is time, k

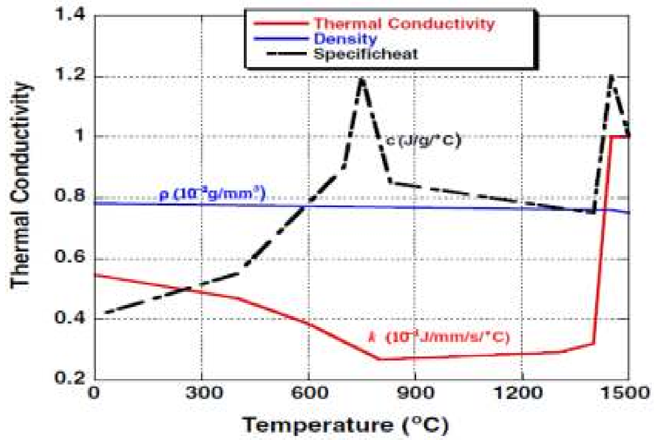

Fig. 2: Temperature dependent thermal properties

Table 2: Temperature dependent mechanical properties of low carbon steel

T [°C]	20	204	316	427	538	649	760	871	982	1093	1204	1316	1427
K [W/m-C°]	59.95	63.7	62.90	61.92	58.36	60.07	44.64	45.78	47	45.66	49.047	49.97	50.87
ρ[kg/m3]	7861	7806	7750	7722.7	7667	7640	7612	7612	7612	7612	7612	7612	7612
σ_y [MPa]	248	200	173	152	117	98	41	21	6.9	5.52	4.83	0.69	0
Et [MPa x103]	11	10.6	10.2	9.6	8.35	5.2	1.9	1.6	1.1	0.759	0.414	0.069	0
E [MPa x103]	207	199	191	179	157	97	35	29	20.7	14.49	8.28	2.07	0
υ	0.3	0.32	0.34	0.3	0.37	0.4	0.4	0.4	0.42	0.423	0.447	0.465	0.46

T is temperature, K is coefficient of heat conduction, ρ is density, σ_y is yield stress, Et is tangent module, E is young module and υ is poison's ratio

is thermal conductivity (W/mm °C), ρ is density, C is specific heat (J/g °C), h is a convection coefficient, β is the Stefan-Boltzman constant and $\in$ is emissivity. Considering a quasi-steady state situation, Eq. (2) can be rewritten in the form of Eq. (4), where u (mm/s) is the velocity in the x-direction.

$$k\frac{\delta^2 T}{\delta x^2} + k\frac{\delta^2 T}{\delta y^2} + k\frac{\delta^2 T}{\delta z^2} - u\frac{\delta Q}{\delta x} = -u\rho C\frac{\delta T}{\delta x} \quad (4)$$

Material model: Figure 2 shows temperature dependent thermal properties of the material (Khurram *et al*., 2011). For interpretation of heat transfer by convection in the weld pool, an exaggerated value of the thermal conductivity is considered for temperatures above the melting point. The latent heat of fusion is combined in the material model by increasing the specific heat at the melting temperature. It is also seen that Young's modulus E, the yield stress and thermal expansion coefficient are primary mechanical properties in the thermo-mechanical analysis. The physical mechanical material properties for low carbon steel are given in Table 2 (Iranmanesh and Darvazi, 2008).

Structural analysis: A non-linear transient structural analysis is conducted just after the thermal analysis. The same half model for thermal analysis is utilized for structural analysis except for the boundary conditions and element type. Symmetrical boundary conditions are applied to simplify the process. SOLID185 is used for 3-D modeling of solid structures. Results of transient thermal analysis are used as body force in the mechanical analysis. The total strain comprises of elastic, plastic and thermal strains as in Eq. (5) (Iranmanesh and Darvazi, 2008).

$$\epsilon = \epsilon^e + \epsilon^p + \epsilon^{th} \quad (5)$$

The elastic strain is modeled using the isotropic Hook's Law with temperature-dependent Young's module and Poisson's ratio. For the plastic strain of the model with yield level of von misses, temperature dependent mechanical properties and hardening linear kinematic model is obtained. Heat strain is calculated using coefficient of thermal expansion given in Table 2.

RESULTS

Welding deformations: Transverse deformation are normal to the weld bead as shown in Fig. 3 and are a result of thermal strains produced during welding. Expansion and contraction during welding in the direction parallel to the welding line causes longitudinal shrinkage in Fig. 4 and 5 represents out of plane deformation which is the basis for angular distortion.

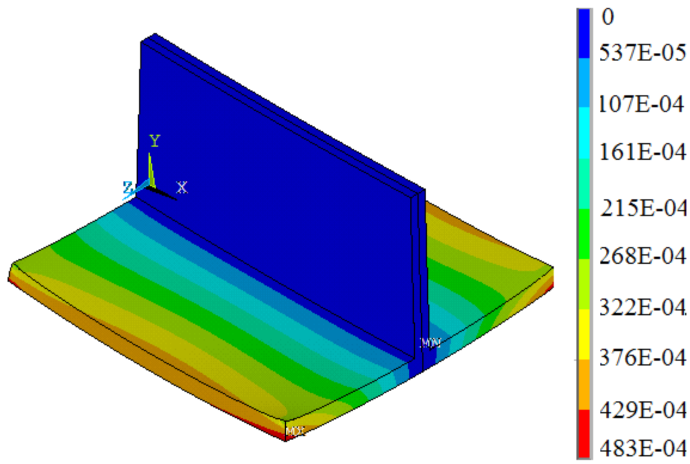

Fig. 3: Deformation in transverse direction

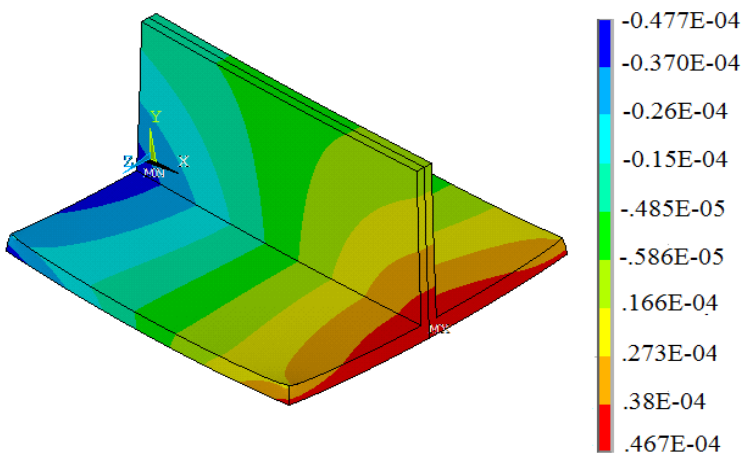

Fig. 4: Deformation in longitudinal direction

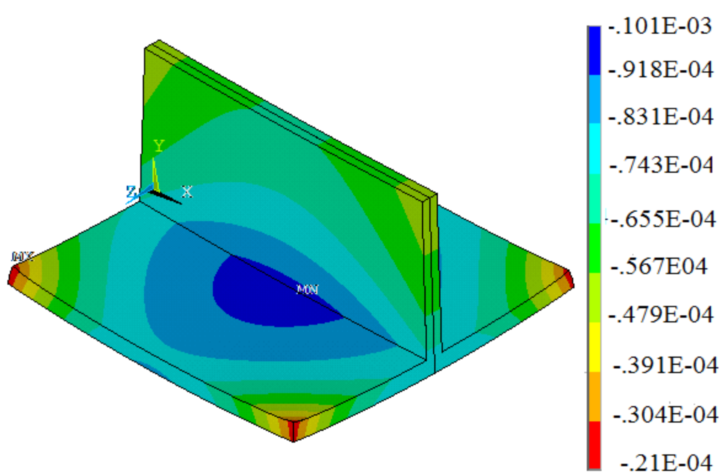

Fig. 5: Out of plane Deformation

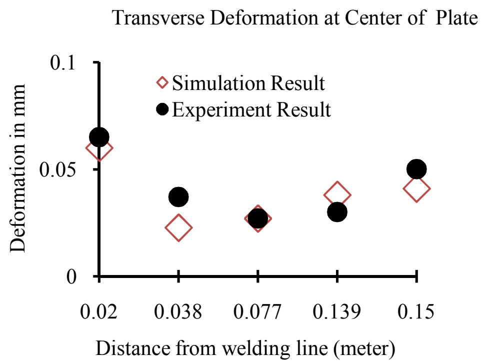

Fig. 6: Comparison of experimental and simulation transverse deformation

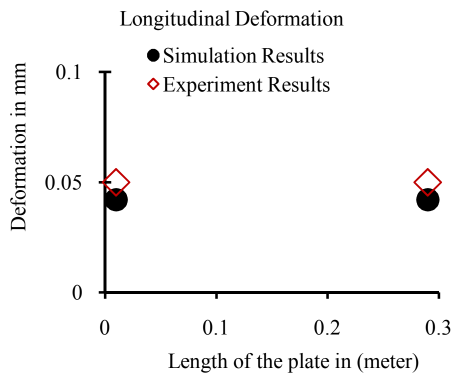

Fig. 7: Comparison of experimental and simulation longitudinal deformation

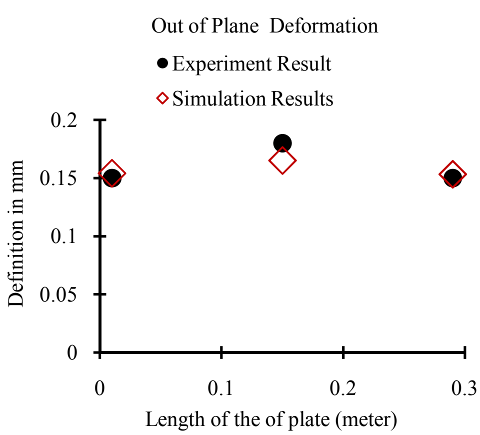

Fig. 8: Comparison of experimental and simulation out of plane deformation

The measured and simulated transverse shrinkage at various points at the mid section of the plate is shown in Fig. 6. Longitudinal deformation at the two extreme ends of the plate are depicted in Fig. 7.

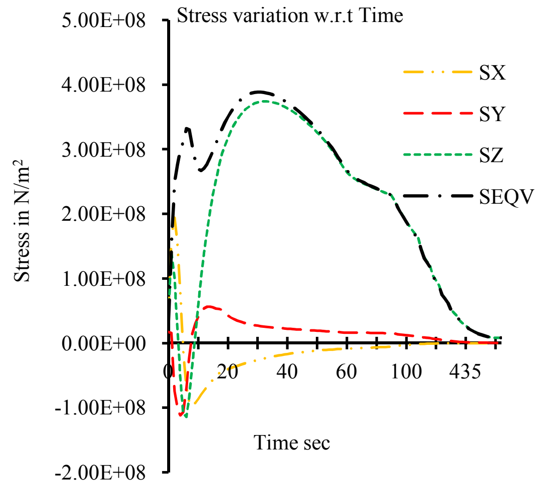

Fig. 9: Stress history of a point at mid thickness

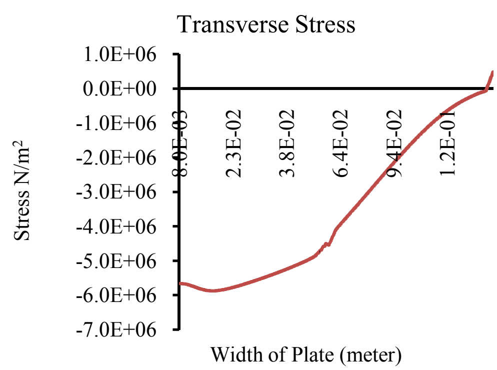

Fig. 10: Transverse stresses at the middle of the plate

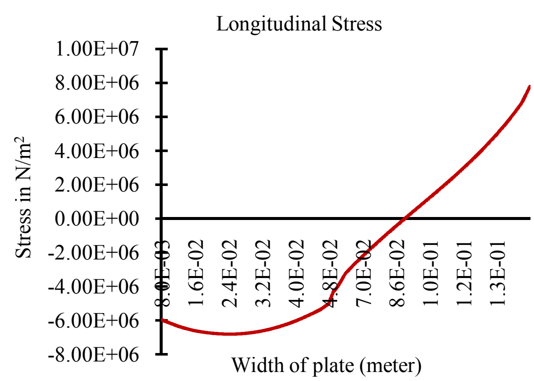

Fig. 11: Longitudinal stress at the middle of the plate

Measured and simulated deformation at various points at mid section of the plate are ploted in Fig. 8. It is evident that the out of plane deformation is more prominent in comparison with the other two deformations.

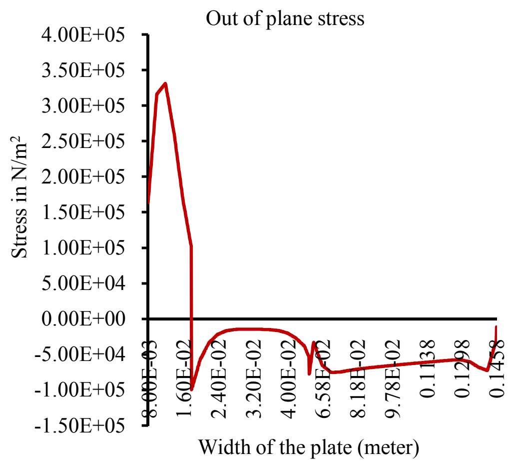

Fig. 12: Out of plane stress at the middle of the plate

Welding residual stresses: Residual stress distribution is not uniform across the thickness of the plate with maximum at the top surface and decreases gradually to minimum at the bottom (Khurram *et al*., 2011). Therefore all stresses are computed at the mid thickness of the plate. Every point within the plate experiences variable stresses during and after welding. Figure 9 shows the stress history of a point at mid thickness of the flange. Results demonstrate that stress is maximum in transverse direction.

Simulation results of transverse and longitudinal residual stresses $(\boldsymbol{\sigma_x}, \boldsymbol{\sigma_z})$ at the flange mid-centerare shown in Fig. 10 and 11, respectively. The residual stresses perpendicular to the flange or out of plane are due to non-uniform expansion and contraction with in the thickness as shown in Fig. 12.

CONCLUSION

This research provides basic theory and instruction to simulate welding residual stresses and deformations in fillet weld joint. Due to symmetry, only half model is considered for analysis. A non- linear transient thermal analysis is performed using a Gaussian distribution based moving heat source. Temperature distribution is computed at each time step independently. Using the results of thermal analysis and applying symmetric boundary conditions, a transient coupled 3D finite element structural analysis is performed. Experiments are also conducted to validate simulation results. Conclusions of this study are summarized as following:

- Simulation results are in a good agreement with experimental values, which prove the authenticity and reliability of the simulation technique.
- Transverse stresses values dominate other stresses through out the welding cycle.
- Transverse and longitudinal stresses are compresive in nature near the weld line.Their value gradually decreases as the distance from the weld line increases and eventually, become tensile near the edges of the plate.
- Out of plane stresses near the weld are are tensile, which gradually decrease and become compressive. However the values are much lower in contrast to other stresses.
- The current method can be used to simulate complex geometries and various welding technologies.

REFERENCES

Barroso, A.J.C., R. Picón, F. París, C. Méndez and I. Unanue, 2010. Prediction of welding residual stresses and displacements by simplified models, experimental validation. Mat. Dsgn., 31(3): 1338-1349.

Camilleri, D., *et al*., 2003. Investigation of Temperature Transients during Flux-Cored CO2/Ar Butt Welding of CMn Steel Plates. METFAB, pp: 107-116.

Camilleri, D., T. Comlekci and T.G.F. Gray, 2005. Computational prediction of out-of-plane welding distortion and experimental investigation. J. Strain Anal., 40(2): 161-170.

Gao, Y. and F. Zhang, 2011. Finite element analysis of simple welding structure. AIMSEC, pp: 3988-3991.

Goldak, J., 2005. Computational Welding Mechanics.

Iranmanesh, M. and A. Darvazi, 2008. Analytical and numerical simulation of temperature field and residual stresses of butt weld in steel plates used in ship manufacturing. Asian J. App. Sce., 1(1): 70-78.

Khurram, A., H. Li, L. Li and S. Khurram, 2011. FE simulation of welding distortion and residual stresses in butt joint using inherent strain. Proceeding of 4th IEEE ICCSIT, pp: 635-640.

Lee, C.H., K.H. Chang and C.Y. Lee, 2008. Comparative study of welding residual stresses in carbon and stainless steel butt welds. J. Engg. Manufacture, 222(12): 1685-1694.

Lindgren, L.E. 2001. Finite element modeling and simulation of welding. J. Therm. Stress., 24(3): 195-231.

Lindgren, L.E. and L. Karlsson, 1988. Deformations and stresses in welding of shell structures, Int. J. Num. Meth. Engg., (25): 635-655.

Moraitis, G.A. and G.N. Labeas, 2009. Prediction of residual stresses and distortions due to laser beam welding of butt joints in pressure vessels. Int. J. Pres. Ves. P., 86: 133-142.

Mollicone, P., D. Camilleri, T.G.F. Gray and T. Comlekci, 2006. Simple thermo-elastic–plastic models for welding distortion simulation. J. Mat. Proces. Tech., 176: 77-86.

Mrvar, P., M. Jožef and S. Kastelic, 2011. Welding sequence definition using numerical calculation. Weld. J., 90:148-151.

Sulaiman, M.S., Y. Manurung, E. Haruman and M.R. Abdul Rahim, 2011. Simulation and experimental study on distortion of butt and T- joints using weld planner. J. Mech. Sce. Tech., 25(10): 2641-2646.

Teng, T., C.P. Fung and P.H. Chang, 2001. Analysis of residual stress and distortions in T-joint fillet welds. Int. J. Press. Vesl. Piping, 78: 523-538.

Ueda, Y. and M.G. Yuan, 1993. Prediction of residual stresses in butt welded plates using inherent strains. J. Engg. Mat. Tech, 115(4): 417-423.

Ueda, Y., Y.C. Kim and M.G. Yuan, 1988. Predicting method of welding residual stress using source of residual stress. J. Japan Weld. Scty, 6(1): 59-64.

Withers, P.J. and H.K.D.H. Bhadeshia, 2001. Residual stress (Part 1- Measurement techniques). Bhad. Mat. Sci. Tech., 17: 355-365.

Xu, J., L. Chen, J. Wang and C. Ni, 2008. Prediction of welding distortion in multi-pass girth-butt welded pipes of different wall thickness. Int. J. Adv. Manuf. Tech., 35: 987-993.